frontiers | Frontiers in Earth Science

TYPE Original Research
PUBLISHED 22 August 2022
DOI 10.3389/feart.2022.890998

OPEN ACCESS

EDITED BY
Pablo Grosse,
Consejo Nacional de Investigaciones Científicas y Técnicas (CONICET), Argentina

REVIEWED BY
Kevin Michael Ward,
South Dakota School of Mines and Technology, United States
Stephanie Prejean,
United States Geological Survey (USGS), United States

*CORRESPONDENCE
Heather McFarlin,
hlmcfarlin@alaska.edu

SPECIALTY SECTION
This article was submitted to Volcanology, a section of the journal Frontiers in Earth Science

RECEIVED 07 March 2022
ACCEPTED 20 July 2022
PUBLISHED 22 August 2022

CITATION
McFarlin H, Thompson G, McNutt SR, Braunmiller J and West ME (2022), Classification of seismic activity at the Lazufre Volcanic System, based on 2011 to 2012 data.
Front. Earth Sci. 10:890998.
doi: 10.3389/feart.2022.890998

Classification of seismic activity at the Lazufre Volcanic System, based on 2011 to 2012 data

Heather McFarlin[1,2]*, Glenn Thompson[1], Stephen R. McNutt[1], Jochen Braunmiller[1] and Michael E. West[2]

[1]School of Geosciences, University of South Florida, Tampa, FL, United States, [2]Geophysical Institute, University of Alaska Fairbanks, Fairbanks, AK, United States

The Lazufre Volcanic System (LVS), on the border of northern Chile and Argentina, is an active complex of two volcanoes, Lastarria to the north and Cordón del Azufre to the south. The LVS is not regularly monitored with any scientific equipment despite being recognized as a top ten volcanic hazard in Argentina by the Observatorio Argentino de Vigilancia Volcánica of the Servicio Geológico y Minero Argentino. The system has shown unusual inflation signatures observed in InSAR but the level of seismic activity and its spatial and temporal distribution were unknown due to the lack of a permanent local seismic network. The PLUTONS Project deployed eight broadband seismic stations throughout the LVS between November 2011 and March 2013. This study shows event locations and types from November 2011 through March 2012. We analyze 591 seismic events within 20 km of Lastarria. Most events cluster tightly beneath Lastarria and almost no activity is observed beneath Cordón del Azufre or the primary inflation center. All events are reviewed manually, and located using a velocity model that assimilates prior studies and accounts for hypocenters within the edifice up to 5 km above sea level. More than 90% of the resulting hypocenters are shallower than 10 km below sea level. The waveforms have characteristics similar to those observed at many other volcanoes, suggesting five classes of events: volcano-tectonic (VT), long-period 1 (LP1), long period 2 (LP2), hybrid (HY), and unknown (X). Frequency-magnitude analysis reveals distinct b-values ranging from 1.2 for VT events to 2.5 for LP1 events. Based on the spatial distribution of events and the b-values, we infer that seismic activity is driven mainly by movement of fluids and gases associated with the regional magma zones and inflation centers. The seismic activity is energetic at times, and quieter at others, suggesting the presence of episodic magmatic and/or hydrothermal activity, focused at Lastarria. Our findings indicate that the previously observed inflation signals are indeed volcanic in origin. These results also demonstrate the potential for success of a future seismic monitoring system and provide a framework for interpreting the subsequent observations, both of which are critical to assessing the volcanic risk of the northern Chile-Argentina region.

KEYWORDS

Lastarria, Lazufre, volcano seismology, Central Andes, PLUTONS project

Introduction

One requirement for a volcanic risk assessment is data showing the baseline level of seismic activity at a volcano. Understanding where, and what types of earthquakes are occurring at a volcano is essential. The Lazufre Volcanic System (LVS, centered at ~25.252°S, 68.514°W; Figure 1), on the border of northern Chile and Argentina, was recently classified as a top ten volcanic hazard in Argentina (Garcia and Badi, 2021), even though the types, locations, and frequency of volcanic earthquakes were unknown.

InSAR studies have shown large deformation signatures at numerous volcanoes in the Central Andes (Pritchard and Simons, 2002). One of the most prominent of these signatures is between two volcanoes, Lastarria to the north and Cordón del Azufre to the south, on the northern border between Chile and Argentina (Figure 1). Pritchard and Simons (2002) refer to the study region as "Lazufre", a blend of the names of the two volcanoes surrounding the deformation. We refer to it as the Lazufre Volcanic System. The LVS is in the Central Volcanic Zone of the Andes, approximately 300 km east of the subduction trench, on the northern edge of the Southern Puna Magma Body (SPMB) and lies in the modern volcanic arc (Bianchi et al., 2013).

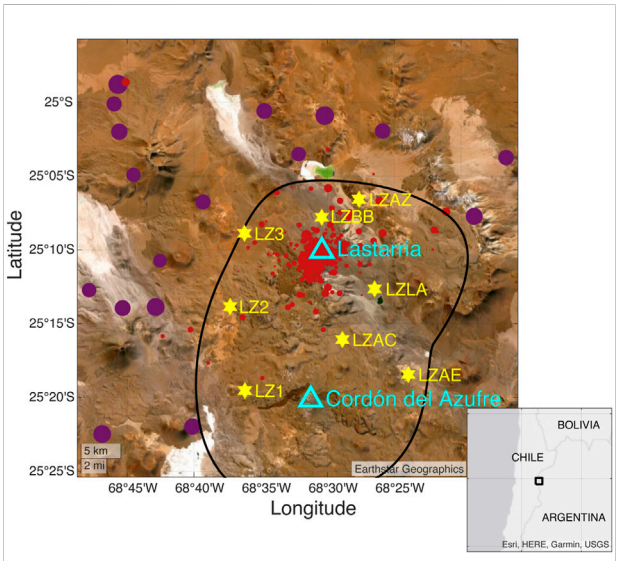

FIGURE 1
Map showing locations of Lastarria and Cordón del Azufre volcanoes (cyan triangles; Smithsonian Global Volcanism Program), seismic stations (yellow stars), regional seismicity (purple circles) and seismic events analyzed and located in this study (red circles). Circle radius is proportional to magnitude, with regional events from M_b3.5 to M_b6.1 from the International Seismology Center from 1960–2020 (ISC, 2022). Black line shows approximate extent of deformation due to LMB, as estimated from Spica et al. (2015). The base map is a satellite image from Earthstar Geographics. Inset map shows location of the main map as a black square on the border between Northern Chile and Argentina (north is up).

The SPMB is a region of partial melt that includes smaller melt bodies such as the Lazufre Magma Body (LMB), the Cerro Galán Magma Body, and the Incahuasi Magma Body (Ward et al., 2013; Ward et al., 2017; Delph et al., 2017; Pritchard et al., 2018). The LMB has been inflating at ~2.5 cm/yr since at least 1998, over an NNE-oriented ellipsoidal region that is ~45 x 37 km^2 (Pritchard and Simons, 2002) and centered at ~25.259°S, ~68.483°W (Henderson et al., 2017). The current hypothesis is that this inflation is due to a magma reservoir at 5–10 km below sea level (bsl) as evidenced by receiver functions (McFarlin et al., 2014), low V_s at ~5 km bsl (Ward et al., 2013) and geobarometry (Stechern et al., 2017); the latter also indicates multiple storage zones at > 20 km depth, likely connected by a system of dikes and sills with the shallower reservoir. While the LMB inflation has been continuous, it does appear to vary by ±1.5 cm in approximately 5–7-year cycles (e.g., Ruch et al., 2009; Henderson and Pritchard, 2013; Pearse and Lundgren, 2013; Remy et al., 2014; Henderson et al., 2017; Pritchard et al., 2018). The current study covers a period of decreased inflation rate of ~1.5 cm/yr, down from the previous years of ~3 cm/yr.

Due to the remoteness of these volcanoes, no permanent geophysical monitoring stations exist. The closest permanent seismic station is GO02, part of the Chilean National Seismic Network, about 110 km west of the LVS. The International Seismological Center (ISC) Bulletin only contains a few regional, mainly intermediate-depth earthquakes in this area above magnitude 3.0, but no small magnitude, shallow events local to the LVS. Recently, because of the large amount of inflation found at this volcanic system, and other research showing the potential for volcanic activity, such as a suggested shallow magma intrusion based on magnetotelluric data (Díaz et al., 2015), the Observatorio Argentino de Vigilancia Volcánica (OAVV) of the Servicio Geológico y Minero Argentino (SEGEMAR) classified Lastarria as a top ten potential hazard in the northern region of Argentina (Garcia and Badi, 2021). Because a detailed study of the seismicity of these volcanoes has never been conducted, the activity levels and states of the volcanoes are essentially unknown.

Despite evidence of inflation, and associated speculation about gas and magma movement in the LVS, there has been no on-site observation of seismic activity to corroborate ongoing volcanic activity and elevated risk at the LVS. Without local seismic records, it is impossible to identify local earthquakes and their spatial and temporal patterns. If Lastarria or Cordón del Azufre are seismically active, then this activity can be used to infer: 1) where, and at what depths, crustal magmatic activity might be most vigorous; 2) whether seismic activity is driven primarily by fluids and gases, or by stresses and tectonics in the surrounding crust; 3) and whether the movement of magma and gas is episodic or more steady state. These questions are societally important because they lay the foundation for any future monitoring efforts and can inform volcanic hazard analyses for the larger region. Here, we present a characterization of

the seismic activity for the LVS based on a 5-month deployment of local seismic stations (Figure 1).

Geologic setting

Lastarria (25.168°S, 68.507°W) and Cordón del Azufre (25.336°S, 68.521°W) are each within 10 km of the inflation center associated with the LMB (Figure 1). Lastarria is more active than Cordón del Azufre and is a polygenetic volcanic complex with a summit at 5,706 m above sea level (asl) (De Silva and Francis, 1991; Tamburello et al., 2014). The volcano consists of four semi-nested craters that trend NNW (approximately perpendicular to the orientation of the NNE-trending LMB inflation signal), with the youngest being the farthest north (De Silva and Francis, 1991). Lastarria is an andesitic-dacitic volcano that has not erupted in 2,500 years (Naranjo, 2010; Lopez et al., 2018), but has four extensive, active fumarole fields with evidence of liquid sulfur flows (Naranjo, 1985; Naranjo, 1988; De Silva and Francis, 1991) and vigorous degassing (Lopez et al., 2018).

Two small and shallow sources of inflation have recently been discovered directly beneath Lastarria, with the sources approximately 4 km asl and 1 km bsl. Both correspond to low velocity zones (decreases in P and S velocities in Figure 2, denoted as ULVZ A and ULVZ B in Figure 3; Spica et al., 2015). The shallower of the two (ULVZ A, ~4 km asl, Figure 3) is thought to be related to the hydrothermal system, with a low Vs. of 1.25 km/s (Figure 2; Spica et al., 2015) and very low resistivity of ~1–10 Ωm (Díaz et al., 2015). The heat flow in this area is high (>700 mW/m^2; Pritchard et al., 2018), and is evident at the surface by fumarole temperatures and liquid sulfur flows (80–408°C; Aguilera et al., 2012; Zimmer et al., 2017; Pritchard et al., 2018). The deeper inflation source from 2 km asl to 1 km bsl (ULVZ B, Figure 3) is thought to be a shallow magma chamber based on low Vs. (1.25 km/s; Spica et al., 2015), low resistivity (~5–10 Ωm, Díaz et al., 2015) and high HCl and HF concentrations, which are indicative of shallow magma degassing (Tamburello et al., 2014; Lopez et al., 2018; Pritchard et al., 2018). This deeper inflation has been modeled as a spherical over-pressurized source that has been inflating at ~9 mm per year since ~2003 over a 6 km^2 area (e.g., Pritchard and Simons, 2002; Froger et al., 2007; Ruch et al., 2009; Pritchard et al., 2018).

Between 2009 and 2012, a change in gas chemistry of the fumaroles from a hydrothermal to a more magmatic signature occurred (Aguilera et al., 2012; Lopez et al., 2018). This might indicate that heat from ascending magma 'dries out' the hydrothermal system, or that ascending magma stalls out and degasses due to isobaric crystallization (Aguilera et al., 2012). Current thoughts are that the Lastarria fumarole fields may serve as a pressure valve for the inflating LMB (Froger et al., 2007; Spica et al., 2015; Pritchard et al., 2018).

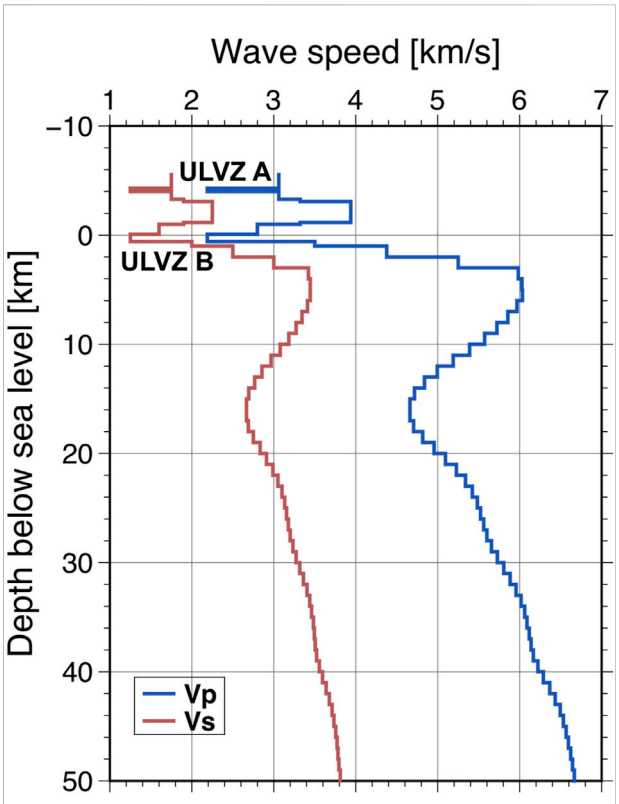

FIGURE 2
Velocity model used in this study, as combined and modified from Ward et al. (2017) and Spica et al. (2015). Red line is the S-wave velocity. Blue line is the P-wave velocity. Depths start at 5.706 km above sea level (at the surface and shown as negative depths). The model includes the two shallow ULVZs (labelled ULVZ A and ULVZ B) from Spica et al. (2015) and a deeper, broad low velocity zone from ~5–33 km bsl based on Ward et al. (2017). Supplementary Table S1 lists Vp, Vs., and Vp/Vs. with depth; Supplementary Table S2 lists alternate model with low velocity zones eliminated.

Cordón del Azufre is also an andesitic-dacitic volcano, with a summit elevation of 5,481 m asl. It is less active than Lastarria, with its most recent eruptions between 0.6 and 0.3 Ma (Naranjo et al., 2018). Activity consisted of pyroclastic and lava flows, and domes, mostly towards the NE side of the volcano (De Silva and Francis, 1991). Each lava flow is less than 1 km in length, but the cluster is large (~45 km^2; De Silva and Francis, 1991) and of a dacitic composition. The older craters of Cordón del Azufre trend N-S, with a total of 4 craters in a 5 km-long chain (De Silva and Francis, 1991).

Data and methods

The PLUTONS project (Pritchard et al., 2018) deployed eight seismic stations in the Lazufre region between November 2011 and March 2013 (Figure 1). Five of these stations, LZAZ, LZBB, LZ3,

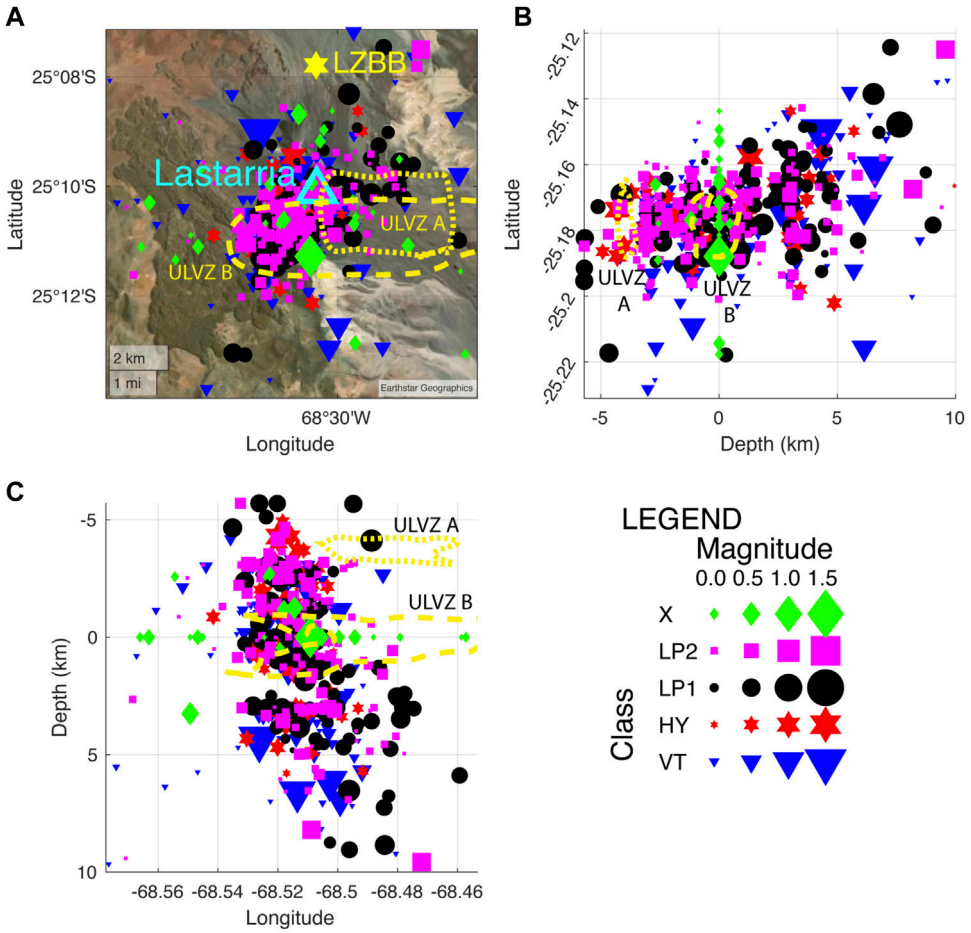

FIGURE 3
Hypocenters of events located in this study, within ~5 km of Lastarria, from 11 November 2011 to 31 March 2012. Symbols indicate event types, and are sized by magnitude, as shown in the legend on the lower right. Ultra-low velocity zones A (ULVZ A) and B (ULVZ B), estimated from Spica et al. (2015) are shown as dotted and dashed yellow lines, respectively. (A) Map view. Lastarria volcano shown as cyan triangle. Cordón del Azufre is off the map, as are the seismic stations except for LZBB. The map is approximately 11 x 11 km and north is up. In (B) Latitude vs. Depth, and (C) Depth vs. Longitude plots. Negative depths are above sea level.

LZ2, LZ1 (all towards the west) consisted of Güralp 3T-120 sec 3-component broadband seismometers with RT-130 digitizers. The remaining three stations, LZLA, LZAC, LZAE (all towards the east) were Güralp 6TD 3-component broadbands with integrated digitizers. A ninth station (LZ6) was installed but was not operational for the entirety of the deployment. In this study, we examine data between November 2011 and March 2012; the remaining data have yet to be analyzed.

We built an initial LVS seismic event catalog using the BRTT Antelope suite (Vernon et al., 2021). We began our analysis by visually inspecting a subset of the waveform data and developing a classification scheme specific for the events observed. We then tuned the Antelope program *dbdetect* STA/LTA (short-term average/long-term average) parameters (Butterworth filter 1.0–20 Hz, STA = 0.5 s, LTA = 60 s, detection "on" threshold = 4.0, detection "off" threshold = 2.0), to capture these events. Auto-locations were computed with the *GENLOC* library (Pavlis et al., 2004), which is packaged with Antelope. We used the velocity model *utu03* (Hutchinson, 2015) for initial locations.

The velocity model used for manual review is a combination of the models from Ward et al. (2017) and Spica et al. (2015) (Figure 2), modified to account for the ~5 km of crust asl. We used the Spica et al. (2015) model for the depths above 3 km bsl and the Ward et al. (2017) model for depths below 3 km bsl. The two studies had different scales and focused on different depths. Combining them thus provides a detailed velocity model for the shallowest depths, and a more generalized model at larger depths (Supplementary Table S1). Both models are V_s models, and we used a constant V_P/V_s ratio of 1.75 to obtain V_P Sea level is chosen as the 0 km reference depth for the combined velocity

model, and the surface in this region is at ~5 km asl, so shallow events have negative depths between -5.6 and 0 km asl. The resulting velocity model includes the two low velocity zones under Lastarria (ULVZ A and ULVZ B) and the deeper low velocities of the LMB (Figures 2, 3).

Manual review of the tuned catalog consisted of visual analysis of each auto-detected event with the Antelope program *dbloc2*, adjusting P and S picks, adding any additional P and S picks, re-locating the event (with *GENLOC*), and re-calculating M_L. We used the zoom function in the *dbpick* window to find where an emergent earthquake signal started and adjusted the P phase pick uncertainty accordingly. We also made use of the Antelope command *dbspgram* to aid in identification of phase arrivals and frequency content of the waveforms. If an S phase was difficult to identify for a given event, then we did not add an S pick to that station for that event. In general, S phase pick uncertainties are larger than those for P phase picks, and the pick phase uncertainty for emergent, low frequency events is higher than for impulsive, high frequency events. The eastern stations (LZLA, LZAC, LZAE) exhibited higher noise levels than the rest of the network. It is unclear whether the higher noise reflects site conditions or the instrumentation. The impact, however, is that phases were more difficult to identify and had larger errors in the east. For some events this introduced large azimuthal gaps and location errors in the east side of the array. Events with fewer than 4 P picks and 3 S picks were rejected. Default *dbevproc* parameters were used to calculate local magnitudes (M_L). Analyses of event counts and event rates were performed with the GISMO Toolbox for MATLAB (Thompson and Reyes, 2018).

Results

Catalog overview

Our final catalog consists of 613 located events between 11 November 2011 and 31 March 2012. Of these, 591 are within 20 km of Lastarria, corresponding to an average of 4.2 events per day within the 142-day period. But activity is episodic; we find an average of 4.8 events per day for the first 59 days, then 0.5 events per day for the next 33 days, and 5.8 events per day for the final 50 days, reaching a maximum of 26 events on 25 March 2012.

Classification scheme

We identified five different classes of event types in our catalog, based on analysis of event waveforms and corresponding spectra. These are in general agreement with terminology and classifications used widely in volcano seismology. There is no single agreed-upon global terminology. Rather, basic event types are identified but local terminology is modified to remedy characteristics of the particular stations, events, and geography. See McNutt et al. (2015) and Wasserman (2012) for reviews.

- Volcano-Tectonic (VT) events show an impulsive P arrival and a clear S wave (Figure 4A), and they have a broad frequency spectrum from ~2–20 Hz (Figure 4B). A total of 202 VT events are in our catalog, an average rate of 1.4 events per day. There is an apparent lull in VT activity from 8 January to 10 February 2012, with only four events in this period (Figure 5). 58% of VT events occurred in the final 50 days.
- Hybrid (HY) events have a high frequency onset, and decay to lower frequencies in the coda (Figures 4C,D). A total of 66 HY events are in our catalog, an average of 0.47 events per day. 68% of HY events occurred in the final 50 days (Figure 5), with only three events between 8 December 2011, and 10 February 2012.
- There are also two types of events with lower frequencies than VT and hybrid events. We termed these two types Long Period 1 (LP1) and Long Period 2 (LP2), based on their frequency content. Both LP types were completely missed by the initial autodetection but were identified visually, and then detected using revised STA/LTA parameters. The S phase picks for the long period events are not true S phases. We put the S pick on the first large amplitude of the event after the initial onset and used *dbspgram* to look at the strength of the frequency content with time to aid in phase identification and event classification.

  LP1 events have a dominant frequency of 3–4 Hz and are monochromatic (Figures 4E,F). A total of 130 LP1 events are in our catalog. The P arrival is emergent (error bars on each P pick are adjusted to account for emergence and uncertainty in arrival onset). The event rate is fairly constant, except for 8 January to 10 February 2012, when only three LP1 events occurred (Figure 5).

  LP2 events are quasi-monochromatic, with a dominant frequency of ~4–6 Hz (Figures 4G,H). A total of 165 LP2 events are in our catalog. 58% of these events occurred before 8 January 2012, and 39% occurred after 10 February 2012 (Figure 5).
- Unknown events: We identified additional events with frequencies and waveforms inconsistent with the classification scheme discussed above. We label these as "X" events. Most have no discernable S phases. Many of these events had a curious, reverse-hybrid look to their waveform with a low frequency onset and high frequency coda. These resemble LP-rockfall events seen at Soufriere Hills Volcano, Montserrat (Luckett et al., 2002), though we have no evidence of a similar mechanism. A total of 50 X events are in our catalog, and examples can be found in Supplementary Figure S7. Their rate of occurrence varied from 0.15 to 0.4 events per day.

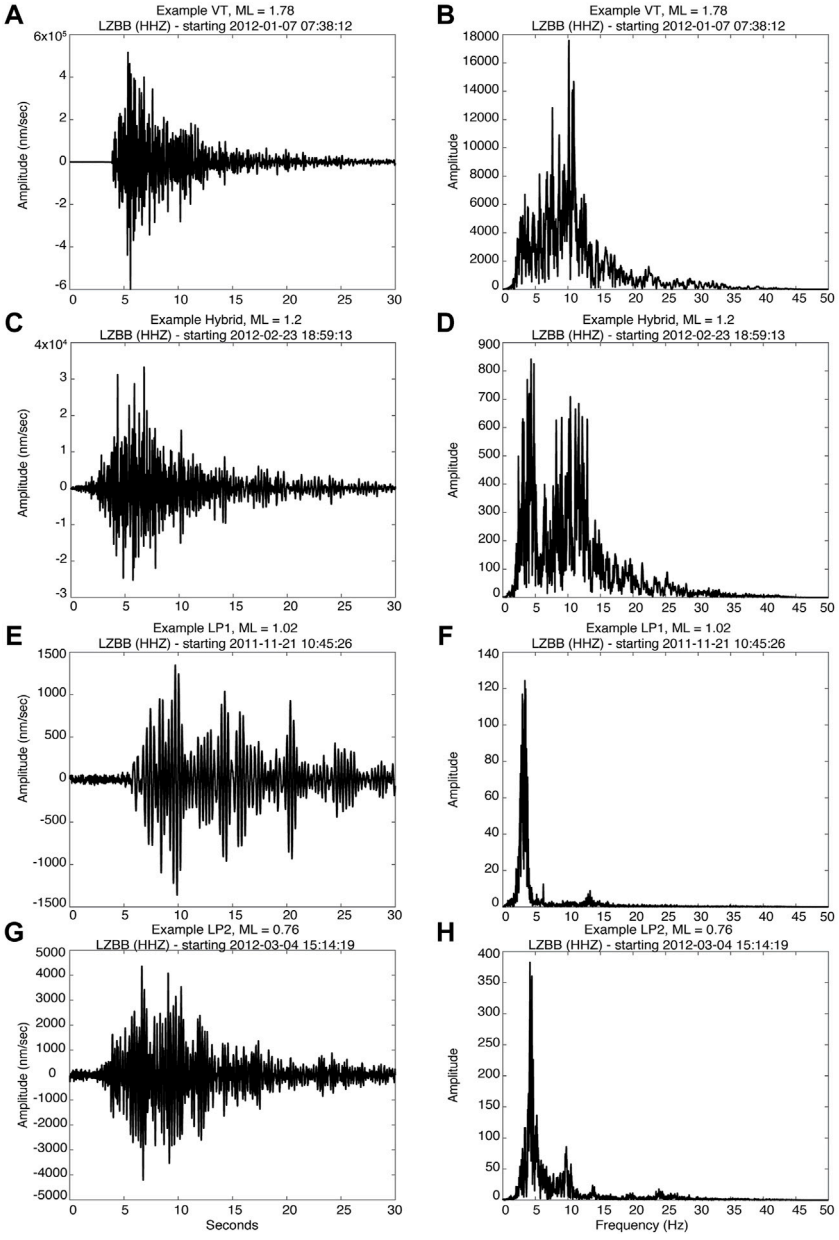

FIGURE 4
Example vertical component waveforms and associated spectra for each event type at station LZBB. Horizontal (E–W) waveforms and associated spectra can be found in Supplementary Figure S7. All waveforms have a time window of 30 s, have been detrended and filtered with a 1 Hz 2-pole high pass filter. **(A)** VT event. Event occurred on 01/07/2012 07:38:12 UTC at 25.1499°S, 68.5262°W, and depth of 4.3 km bsl, with M_L = 1.78. **(B)** Spectra from seismogram in **(A)**. **(C)** Hybrid event. Event occurred on 02/23/2012 18:59:13 UTC at 25.1737°S, 68.5198°W, and depth of 4.3 km asl, with M_L = 1.2. **(D)** Spectra from seismogram in **(C)**. **(E)** Long Period Type 1 (LP1) event. Event occurred on 11/21/2011 10:45:26 UTC at 25.1478°S, 68.4311°W, and depth of 7.6 km bsl, with M_L = 1.02. **(F)** Spectra from seismogram in **(E)**. **(G)** Long Period Type 2 (LP2) event. Event occurred on 03/04/2012 15:14:19 UTC at 25.1692°S, 68.5030°W, and depth of 2.9 km bsl, with M_L = 0.76. **(H)** Spectra from seismogram in **(G)**.

Hypocenters

Hypocenters cluster close to Lastarria (Figures 1, 3, Supplementary Figure S9) and appear to extend from its summit down to approximately the top of the LMB at ~10 km bsl (Supplementary Figure S8) with 90% of events shallower than 6 km bsl and 96.5% shallower than 10 km bsl. The average epicenter of all events is at 25.174°S, 68.514°W (Table 1), which is <1 km southwest of the summit of Lastarria. Of the 613 events in our catalog, 591 are within 20 km, 581 are within 10 km, and 540 are within 5 km of the average epicenter indicating tight clustering. Generally, events trend further to the northeast with increasing

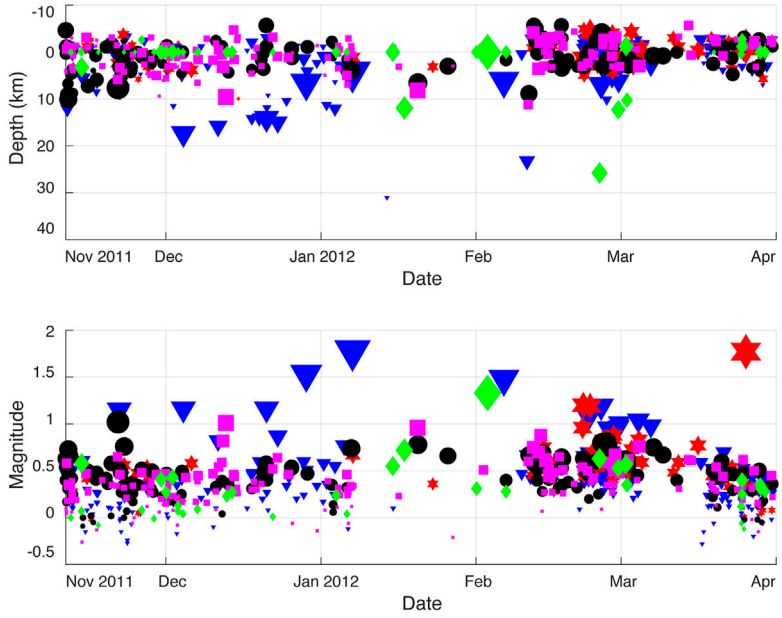

FIGURE 5
Time series of depth and magnitude for events. Symbols and colors depict event types and are the same as in Figure 3. There is an apparent lull in activity across all event types from early January to early February 2012.

TABLE 1 Summary event catalog statistics by event type. Column 2: Number of events within 20 km horizontal distance of the average epicenter (25.174°S, 68.514°W). Column 3: Mean residual time errors between observed and predicted phase arrival times. Columns 4–6: Mean latitude, longitude, and depth of all events (per event type). Column 7–9: Largest event M_L, Mc, and b-value. Plus/minus errors represent one standard deviation. No b-value was estimated for X events due to sample size.

Type	No. of events	Residual (s)	Latitude (°S)	Longitude (°W)	Depth (km)	Largest M_L (±0.1)	Mc (±0.1)	b-value
VT	191	0.48	25.173 ± 0.026	68.518 ± 0.037	1.6 ± 5.1	1.8	0.2	1.2 ± 0.1
Hybrid	66	0.43	25.175 ± 0.010	68.513 ± 0.023	0.2 ± 3.2	1.8	0.5	1.6 ± 0.2
LP1	130	0.39	25.173 ± 0.014	68.509 ± 0.015	0.9 ± 3.1	1.0	0.5	2.5 ± 0.2
LP2	164	0.40	25.174 ± 0.012	68.513 ± 0.015	0.2 ± 3.1	1.0	0.3	1.8 ± 0.1
X	40	0.67	25.178 ± 0.046	68.525 ± 0.047	1.3 ± 5.0	1.3	N/A	N/A
All	591	0.45	25.174 ± 0.021	68.515 ± 0.028	0.9 ± 4.0	1.8	0.3	1.5 ± 0.1

depth, consistent with a feature dipping at about 20° to the vertical. We found little to no activity in the immediate vicinity of Cordón del Azufre; this result does not appear to be an artifact of the network geometry. Most VT, HY, LP1 and LP2 events have 4–6 P-phase picks, and 4–6 S-phase picks (Figure 6, Supplementary Figures S1–S5). Only 2.5% of these events locate further south than 25.2°S.

Hypocenter distributions and uncertainties show little dependence on event class (Table 1; Supplementary Figure S9). The epicentral distributions of each event class are statistically identical. For example, the average epicenter of VT events is within 0.4 km of the average epicenter of HY events, which is only 10–20% of one standard deviation. Mean differences between predicted and observed arrival times range from 0.39 s for LP1 events to 0.48 s for VT events, again showing little variation.

Depth distributions also overlap but show some separation. The average depths are 0.2 km for HY and LP2 events, 0.9 km for LP1 events, and 1.6 km for VT events. These mean depth differences are well within one standard deviation (3.1–5.2 km; Table 1). 95% of HY events are shallower than 5.0 km bsl, increasing to 5.9 km for LP2 events, 6.8 km for LP1 events, and 12.0 km for VT events.

Only 14 of 50 X events have discernable S-phases, so X hypocenters are poorly constrained (particularly depths). For X events without S-phases, we fixed depths to 0 km. We also tried fixing depths to -5 km, but then only eight X

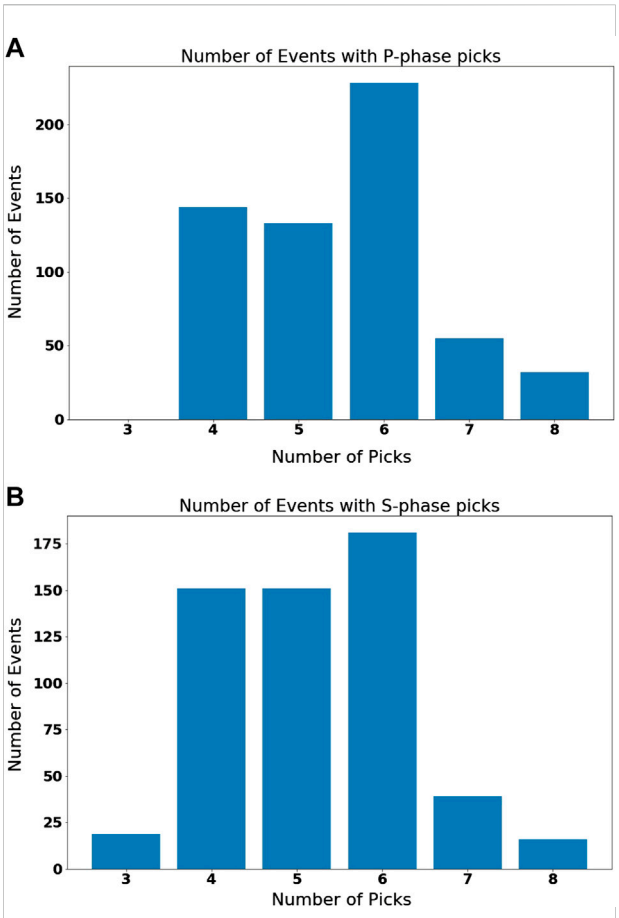

FIGURE 6
Histograms showing the number of events versus number of P phase picks **(A)**, and S phase picks on the **(B)**, for all event types. A breakdown by event type can be found in the Supplementary Figures S1–S5.

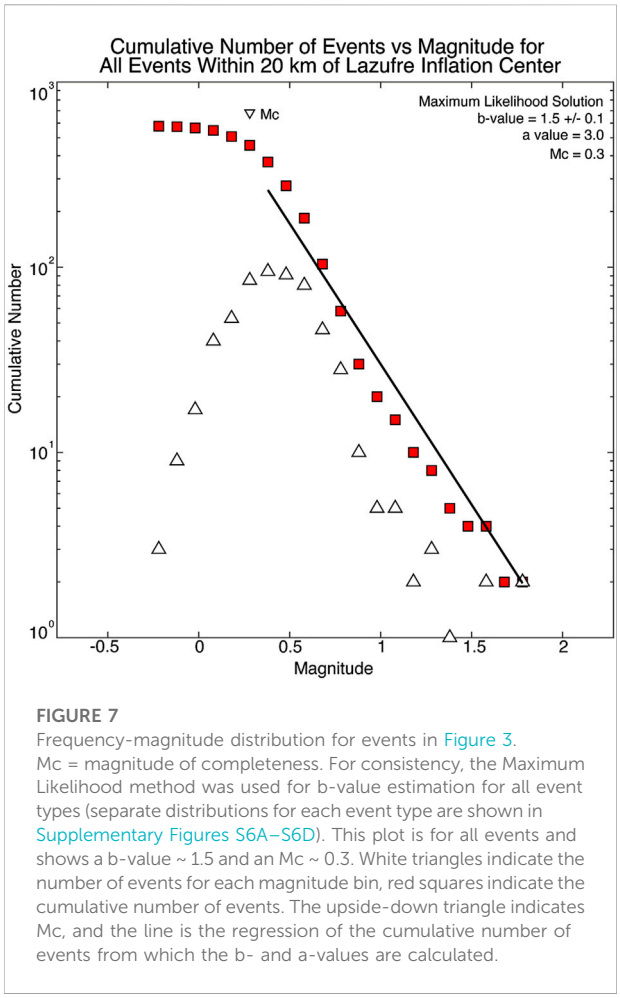

FIGURE 7
Frequency-magnitude distribution for events in Figure 3. Mc = magnitude of completeness. For consistency, the Maximum Likelihood method was used for b-value estimation for all event types (separate distributions for each event type are shown in Supplementary Figures S6A–S6D). This plot is for all events and shows a b-value ~ 1.5 and an Mc ~ 0.3. White triangles indicate the number of events for each magnitude bin, red squares indicate the cumulative number of events. The upside-down triangle indicates Mc, and the line is the regression of the cumulative number of events from which the b- and a-values are calculated.

events locate within the Figure 1 region, suggesting these events are not related to surficial processes.

Magnitudes

Local magnitudes (M_L) in our catalog range from −0.3 to 1.8. The largest VT was a M_L=1.8 event in early January 2012 (Figure 5). The largest hybrid event was also M_L=1.8 (in late March 2012). The largest LP1 and LP2 events were only M_L=1.0.

All b-values in this study (Table 1; Figure 7, Supplementary Figure S6) were calculated using the maximum likelihood solution for curve-fitting. The b-value for VT events is 1.2 ± 0.1 (Supplementary Figure S6A). This is a typical value for VT earthquakes near volcanoes (i.e., Roberts et al., 2015; McNutt, 1996). We estimate a magnitude of completeness (Mc) of 0.2 for VT events. The b-value for hybrid events is 1.6 ± 0.2 with Mc = 0.5 ± 0.1 (Supplementary Figure S6B). The b-value for LP1 events is 2.5 ± 0.2, with Mc = 0.5 ± 0.2 (Supplementary Figure S6C). This b-value is quite high but is comparable to LP events at other volcanoes (Glazner and McNutt, 2021). The b-value for LP2 events is 1.8 ± 0.1 with Mc=0.3 ± 0.1 (Supplementary Figure S6D). These b-values may not be statistically robust given the small spread in M_L.

We note that there is an inverse correlation between b-value and frequency content: LP1 events have the lowest frequency content, and a high b-value. The opposite is true for VT events.

Discussion

The manually reviewed events occurring within the LVS from November 2011 through March 2012 mainly occur in a 5-km-radius cylindrical zone whose axis is just southwest of the Lastarria summit at the surface, dipping to the NE at about 20° off vertical with increasing depth. The shallow events near and southwest of Lastarria cluster close to the shallow magma chambers that have been identified from ambient seismic noise analysis (Spica et al., 2015) and resistivity modeling of magnetotelluric data (C1 and C2 low resistivity

anomalies, Díaz et al., 2015). The C1 anomaly of Díaz et al. (2015) is the shallower of the two, extending down to approximately 4 km asl and is centered around Lastarria. This coincides with the ULVZ A of Spica et al. (2015). Díaz et al. (2015) attributes this upper body to fumarolic activity. The C2 resistivity anomaly of Díaz et al. (2015) is deeper, extending to 2–3 km bsl south of Lastarria. This is coincident with the ULVZ B of Spica et al. (2015), and Díaz et al. (2015) attribute C2 to magmatic fluids, which they speculate are heating fumaroles for the C1 body. Without clear supporting evidence, we suggest the event locations in map and cross-sectional views are consistent with activity on a series of dikes that extend from near the Lastarria summit to the shallow magma chamber and perhaps down to the ceiling at the northern edge of the Lazufre inflation body (Figure 3). VT events are on average deeper than low frequency events (HY, LP1, and LP2) with 5% of VT events deeper than 12 km bsl, and 5% of low frequency events deeper than 5.8 km bsl.

The epicentral locations are stable, but depths vary depending on the velocity model as is common. We found relatively few hypocenters with depths of 0–2 km bsl (Figure 3, Supplementary Figure S8). This 'depth gap' may be related to ULVZ B which extends from -1 to 1 km depth in our model. To examine if this is real, we relocated all hypocenters based on an alternate velocity model that eliminates ULVZ A and B (Supplementary Table S2). Not surprisingly, this alternate model pushed hypocenters an average of 1.7 km deeper (from 0.9 to 2.6 km bsl) and 5% of events are deeper than 11.5 km, since wave speeds are on average higher. The depth gap is reduced, which suggests it is an artifact of the presence of the low-velocity zone in the model. Crucially however, the epicenters do not change much between the two velocity models. Our choice for the shallow part of the velocity model is based on the ULVZs identified by Spica et al. (2015) directly beneath Lastarria. These ULVZs have limited spatial extent such that some, but not all, rays from events to stations pass through them (Supplementary Figure S10). The "true" depth distribution is thus likely a mix of results shown for the two velocity models—the two models likely represent endmembers of the possible model space (Supplementary Figures S11, S12). Since we are using a 1D velocity model in a region with 3D properties, a 3D velocity model with topography could potentially provide better resolved hypocenters but is not trivial to derive or use for the LVS given the scant data.

Seismicity was relatively high from November 2011 to early January 2012, and from mid-February until 31 March 2012 (Figure 5). This contrasts with the period from mid-January to mid-February 2012, when the event rate was 5-times lower. The network operations did not change in any significant way throughout the study period and the observed lull in activity is a real feature. This suggests an episodic nature of activity that likely reflect changes in the magmatic system at depth, indicating that the system itself is not in steady state, resulting in a variable stress/strain environment. This perhaps suggests that all the seismicity is responding to the same external events, such as pulses of magma injection or gas release.

The b-value for the entire catalog is approximately b=1.5 ± 0.1 (Figure 7) and Mc is approximately 0.3 ± 0.1. In general, the b-value is a useful metric to characterize groups of earthquakes. The b-value for tectonic earthquakes is generally ~1.0 whereas volcanoes often show higher values. Complementary lab studies show that b-values are affected by fluids (Wyss, 1973), thermal gradients (Warren and Latham, 1970), stresses (Scholz, 1968), and material heterogeneities (Mogi, 1962), so we can use b-values to make inferences about the state of the crust where earthquakes occur. See Glazner and McNutt (2021) for a recent review and compilation. For the LVS, the VT events have a b-value of 1.2, near the worldwide tectonic average, and likely represent shear failure on faults. The hybrid, LP1 and LP2 events have higher b-values of 1.6–2.5 suggesting the presence of mobile fluids, as supported by active fumarole fields and overall high heat flow in the LVS (Pritchard et al., 2018).

The high b-values across three event types (Figure 7, Supplementary Figure S6) provide further support for an area with a high thermal gradient (Wiemer and McNutt, 1997), or alternatively with either a low stress environment or a highly fractured heterogeneous area (i.e., Eyre and van der Baan, 2015; Schorlemmer et al., 2005; Mogi, 1962). The seismograms within each event type are not identical, indicating that the events are occurring in different places and are not repetitive. Thus, we envision a plexus of cracks, dikes, and/or sills near each other, but cannot resolve this with our data.

Current volcanic activity at the LVS consists of seismicity, extensive and highly active fumarole fields, deformation, and degassing. Gas compositions changed between 2009 and 2012 from a hydrothermal signature to a magmatic signature (Lopez et al., 2018). This is the same time frame that the inflation rate of the deeper mush body, the Lazufre Magma Body (LMB), decreased by half (Henderson et al., 2017; Lopez et al., 2018, Pearse and Lundgren, 2013) perhaps suggesting that ascending magma is stalling out and degasses due to isobaric crystallization (Aguilera et al., 2012). However, without concurrent long-term geophysical and geochemical monitoring, a deeper understanding of the state of the LVS might be out of reach, and a full volcanic risk assessment for this region cannot be made with confidence.

Summary and conclusion

We conducted the first study of seismic activity at the LVS based on local observations. No information about the level of activity or its distribution with respect to the Lastarria and Cordón del Azufre volcanic centers or to an InSAR-observed inflation center located between the volcanoes existed prior to our study. Our ~5-month catalog from November 2011 to March 2012 includes 591 events within 20 km of Lastarria corresponding to about four events per day. The seismic events cluster close to the summit of Lastarria and occur mainly at depth from ~5 km asl to ~6 km bsl (Figure 3). We find little to no evidence for seismicity directly beneath the

Cordón del Azufre volcano and the Lazufre Magma Body inflation center (about mid-way between Lastarria and Cordón del Azufre).

Lastarria is seismically active, and we observed different event types that are characteristic of seismicity at many volcanoes. Our event classes consist of VT, Hybrid, and long period LP1 and LP2 events, all of which tend to occur close to Lastarria above the top of the northern edge of the inflation due to the Lazufre Magma Body (LMB). We found a lull in activity across all event types from mid-January to mid-February 2012 (Figure 5) suggesting the magmatic system is not in steady state. This perhaps indicates that all seismicity might be responding to the same external events, such as episodic pulses of magma injection or gas release at depth beneath the LVS.

The locations of the various events are consistent with the idea that the LMB is "feeding" the shallow, localized inflation center active beneath the summit of Lastarria. These events could be indicative of fluid movement through a series of dikes from the LMB up to the summit of Lastarria (Figure 3). Supporting evidence includes: 1) event depths bottoming out near the top of the LMB (~10 km bsl), with 95% of events being shallower than 6 km depth, 2) most events locating close to Lastarria, rather than to Cordón del Azufre, and are coinciding with previously imaged shallow magma bodies, and 3) high b-values for HY, LP1, and LP2 events, indicating the presence of mobile fluids.

Future work could include identification of additional events (e.g., using cross-correlation, machine learning) to improve the statistical significance of parameters in Table 1 (e.g., b-values) and estimation of 'X' event mechanisms to understand their sources. Relative event relocation (e.g., HypoDD) could be used to delineate boundaries of potential magma/mush bodies or pipes/conduits. Similarly, analysis of the radiation patterns of low frequency events, and modeling based on cracks or pipes could improve understanding of the plumbing system of the LVS. Future seismic studies could include more stations for better network geometry.

Our study shows that the LVS is an active volcanic system that undergoes episodic changes in seismicity. Results from seismicity analysis presented here, combined with observed cycles of varying inflation rates from InSAR and changes in gas composition from geochemical studies, highlight the dynamic nature of the system and the importance for continued and improved long-term monitoring efforts of the LVS. Such efforts are crucial to improve understanding of the volcanic hazards for the larger region.

Data availability statement

The raw data supporting the conclusion of this article will be made available by the authors, without undue reservation.

Author contributions

HM performed the bulk of this work as part of her dissertation. GT wrote code, provided Antelope support, and prepared Figures 1, 3, 5 using GISMO, a seismic toolbox for MATLAB (Thompson and Reyes, 2018). GT, SM, JB, and MW provided funding, training, mentorship, and edited the manuscript.

Funding

Partial funding was provided by the NSF Continental Dynamics Program via a subcontract from UAF to USF, with the project #0909254.

Acknowledgments

The authors would like to acknowledge Matt Gardine for extensive assistance with the BRTT Antelope Suite, along with Alexandra Farrell, Lea Gardine, Dara Merz, and Danielle Molisee for discussions, technical expertise with MATLAB programming, and moral support. Scott Stihler is acknowledged for showing the "proper way" to locate low frequency volcanic events. Jamie Farquharson is acknowledged for processing and providing precipitation data in the Supplement. The authors thank Pablo Grosse for guest editing this special issue, and the two reviewers for their kind and helpful comments.

Conflict of interest

The authors declare that the research was conducted in the absence of any commercial or financial relationships that could be construed as a potential conflict of interest.

Publisher's note

Supplementary material

The Supplementary Material for this article can be found online at: https://www.frontiersin.org/articles/10.3389/feart.2022.890998/full#supplementary-material

References

Aguilera, F., Tassi, F., Darrah, T., Moune, S., and Vaselli, O. (2012). Geochemical model of a magmatic-hydrothermal system at the Lastarria volcano, northern Chile. *Bull. Volcanol.* 74, 119–134. doi:10.1007/s00445-011-0489-5

Bianchi, M., Heit, B., Jakovlev, A., Yuan, X., Kay, S. M., Sandvol, E., et al. (2013). Teleseismic tomography of the southern Puna plateau in Argentina and adjacent regions. *Tectonophysics* 586, 65–83. doi:10.1016/j.tecto.2012.11.016

De Silva, S. L., and Francis, P. (1991). *Volcanoes of the central Andes*, 219. Berlin: Springer-Verlag.

Delph, J. R., Ward, K. M., Zandt, G., Ducea, M. N., and Beck, S. L. (2017). Imaging a magma plumbing system from MASH zone to magma reservoir. *Earth Planet. Sci. Lett.* 457, 313–324. doi:10.1016/j.epsl.2016.10.008

Díaz, D., Heise, W., and Zamudio, F. (2015). Three-dimensional resistivity image of the magmatic system beneath Lastarria volcano and evidence for magmatic intrusion in the backarc (northern Chile). *Geophys. Res. Lett.* 42, 5212–5218. doi:10.1002/2015GL064426

Eyre, T. S., and van der Baan, M. (2015). Overview of moment-tensor inversion of microseismic events. *Lead. Edge* 34 (8), 882–888. doi:10.1190/tle34080882.1

Froger, J.-L., Rémy, D., Bonvalot, S., and Legrand, D. (2007). Two scales of inflation at Lastarria-Cordón del Azufre volcanic complex, Central Andes, revealed from ASAR-ENVISAT interferometric data. *Earth Planet. Sci. Lett.* 255, 148–163. doi:10.1016/j.epsl.2006.12.012

Garcia, S., and Badi, G. (2021). Towards the development of the first permanent volcano observatory in Argentina. *Volcanica* 4 (S1), 21–48. doi:10.30909/vol.04.s1.2148

Glazner, A. F., and McNutt, S. R. (2021). Relationship between dike injection and b-value for volcanic earthquake swarms. *JGR. Solid Earth* 126, 12. doi:10.1029/2020JB021631

Henderson, S. T., Delgado, F., Elliot, J., Pritchard, M. E., and Lundgren, P. R. (2017). Decelerating uplift at Lazufre volcanic center, Central Andes, from A.D. 2010 to 2016, and implications for geodetic models. *Geosphere* 13, 1489–1505. doi:10.1130/GES01441.1

Henderson, S. T., and Pritchard, M. E. (2013). Decadal volcanic deformation in the Central Andes Volcanic Zone revealed by InSAR time series. *Geochem. Geophys. Geosyst.* 14, 1358–1374. doi:10.1002/ggge.20074

Hutchinson, L. (2015). Double-difference relocation of earthquakes at Uturuncu volcano, Bolivia, and Interior Alaska. dissertation. Fairbanks: University of Alaska Fairbanks.

International Seismological Centre (2022). *On-line Bulletin*. Thatcham: Berkshire. doi:10.31905/D808B830

Lopez, T., Aguilera, F., Tassi, F., Maarten de Moor, J., Bobrowski, N., Aiuppa, A., et al. (2018). New insights into the magmatic-hydrothermal system and volatile budget of Lastarria volcano, Chile: integrated results from the 2014 IAVCEI CCVG 12th volcanic gas workshop. *Geosph. (Boulder).* 14, 983–1007. doi:10.1130/GES01495.1

Luckett, R., Baptie, B., and Neuberg, J. (2002). The relationship between degassing and rockfall signals at Soufriere Hills Volcano, Montserrat. *Geol. Soc. Lond. Memoirs* 21, 1. doi:10.1144/GSL.MEM.2002.021.01.28

McFarlin, H. L., Christensen, D. H., Thompson, G., McNutt, S. R., Ryan, J. C., Ward, K. M., et al. (2014). Receiver Function Analyses of Uturuncu Volcano, Bolivia and Lastarria/Cordon del Azufre Volcanoes, Chile. *AGU Fall Meet. Abstr.* 2014, V31E–V4792.

McNutt, S. R. (1996). "Seismic monitoring and eruption forecasting of volcanoes: a review of the state-of-the-art and case histories," in *Monitoring and mitigation of volcano hazards* (Berlin, Heidelberg: Springer). doi:10.1007/978-3-642-80087-0_3

McNutt, S. R., Thompson, G., Johnson, J., De Angelis, S., and Fee, D. (2015). "Seismic and infrasonic monitoring," in *The encyclopedia of volcanoes* (New York, NY: Academic Press), 1071–1099.

Mogi, K. (1962). On the time distribution of aftershocks accompanying the recent major earthquakes in and near Japan. *Bull. Earthq. Res. Inst. Univ. Tokyo* 40 (1), 107–124.

Naranjo, J. A. (1988). Coladas de azufre de los volcanes Lastarria y bayo en el norte de Chile: reología, génesis e importance en geología planetaria. *Rev. Geol. Chile* 15 (1), 3–12.

Naranjo, J. A. (2010). *Geología del Complejo Volcánico Lastarria, Región de Antofagasta*. Santiago: Servicio Nacional de Geología y Minería, Carta Geológica de Chile. 72. 1:250,000 scale, 1 sheet.

Naranjo, J. A. (1985). Sulphur flows at Lastarria volcano in the north Chilean Andes. *Nature* 313, 778–780. doi:10.1038/313778a0

Naranjo, J. A., Villa, V., Ramírez, C., and Ramirez, C. A. (2018). Miocene to Holocene geological evolution of the Lazufre segment in the Andean volcanic arc. *Geosph. (Boulder).* 14, 47–59. doi:10.1130/GES01352.1

Pavlis, Gary L., Vernon, F., Harvey, D., and Quinlan, D. (2004). The generalized earthquake-location (GENLOC) package: an earthquake-location library. *Comput. Geosciences* 30, 1079–1091. doi:10.1016/j.cageo.2004.06.010

Pearse, J., and Lundgren, P. (2013). Source model of deformation at Lazufre volcanic center, Central Andes, constrained by InSAR time series. *Geophys. Res. Lett.* 40, 1059–1064. doi:10.1002/grl.50276

Pritchard, M. E., de Silva, S. L., Michelfelder, G., Zandt, G., McNutt, S. R., Gottsmann, J., et al. (2018). Synthesis: plutons: investigating the relationship between pluton growth and volcanism in the central Andes. *Geosph. (Boulder).* 14, 954–982. doi:10.1130/GES01578.1

Pritchard, M. E., and Simons, M. (2002). A satellite geodetic survey of large-scale deformation of volcanic centres in the central Andes. *Nature* 418, 167–171. doi:10.1038/nature00872

Remy, D., Froger, J. L., Perfettini, H., Bonvalot, S., Gabalda, G., Albino, F., et al. (2014). Persistent uplift of the Lazufre volcanic complex (Central Andes): new insights from PCAIM inversion of InSAR time series and GPS data. *Geochem. Geophys. Geosyst.* 15, 3591–3611. doi:10.1002/2014GC005370

Roberts, N. S., Bell, A. F., and Main, I. G. (2015). Are volcanic seismic b-values high, and if so when? *J. Volcanol. Geotherm. Res.* 308, 127–141. doi:10.1016/j.jvolgeores.2015.10.021

Ruch, J., Manconi, A., Zeni, G., Solaro, G., Pepe, A., Shirzaei, M., et al. (2009). Stress transfer in the Lazufre volcanic area, central Andes. *Geophys. Res. Lett.* 36, L22303. doi:10.1029/2009GL041276

Scholz, C. H. (1968). Microfractures, aftershocks, and seismicity. *Bull. Seismol. Soc. Am.* 58 (3), 1117–1130.

Schorlemmer, D., Wiemer, S., and Wyss, M. (2005). Variations in earthquake-size distribution across different stress regimes. *Nature* 437 (7058), 539–542. doi:10.1038/nature04094

Spica, Z., Legrand, D., Iglesias, A., Walter, T. R., Heimann, S., Dahm, T., et al. (2015). Hydrothermal and magmatic reservoirs at Lazufre volcanic area, revealed by a high-resolution seismic noise tomography. *Earth Planet. Sci. Lett.* 421, 27–38. doi:10.1016/j.epsl.2015.03.042

Stechern, A., Just, T., Holtz, F., Blume-Oeste, M., and Namur, O. (2017). Decoding magma plumbing and geochemical evolution beneath the Lastarria volcanic complex (northern Chile)—evidence for multiple magma storage regions. *J. Volcanol. Geotherm. Res.* 338, 25–45. doi:10.1016/j.jvolgeores.2017.03.018

Tamburello, G., Hansteen, T. H., Bredemeyer, S., Aiuppa, A., and Tassi, F. (2014). Gas emissions from five volcanoes in northern Chile and implications for the volatiles budget of the Central Volcanic Zone. *Geophys. Res. Lett.* 41, 4961–4969. doi:10.1002/2014GL060653

Thompson, G., and Reyes, C. (2018). Gismo - a seismic data analysis toolbox for MATLAB (Version 1.20b) [software package]. Available at: http://geoscience-community-codes.github.io/GISMO/(Accessed Feb 11, 2022). doi:10.5281/zenodo.1404723

Vernon, F., Lindquist, K., and Harvey, D. (2021). Antelope 5.11. [software package]. Available at: https://brtt.com/software/latest-release/(Accessed February 13, 2022).

Ward, K. M., Delph, J. R., Zandt, G., Beck, S. L., and Ducea, M. N. (2017). Magmatic evolution of a Cordilleran flare-up and its role in the creation of silicic crust. *Sci. Rep.* 7, 9047. doi:10.1038/s41598-017-09015-5

Ward, K. M., Porter, R. C., Zandt, G., Beck, S. L., Wagner, L. S., Minaya, E., et al. (2013). Ambient noise tomography across the central Andes. *Geophys. J. Int.* 194, 1559–1573. doi:10.1093/gji/ggt166

Warren, N. W., and Latham, G. V. (1970). An experimental study of thermally induced microfracturing and its relation to volcanic seismicity. *J. Geophys. Res.* 75 (23), 4455–4464. doi:10.1029/jb075i023p04455

Wasserman, J. (2012). "volcano seismology," in *New Manual of seismological observatory practice 2 (NMSOP-2)*. Editor P. Bormann (Potsdam: Deutsches GeoForschungsZentrum GFZ), 1–77. doi:10.2312/GFZ.NMSOP-2_ch13

Wiemer, S., and McNutt, S. R. (1997). Variations in the frequency-magnitude distribution with depth in two volcanic areas: Mount St. Helens, Washington and Mt. Spurr, Alaska. *Geophys. Res. Lett.* 24 (2), 189–192. doi:10.1029/96gl03779

Wyss, M. (1973). Towards a physical understanding of the earthquake frequency distribution. *Geophys. J. Int.* 31 (4), 341–359. doi:10.1111/j.1365-246x.1973.tb06506.x

Zimmer, M., Walter, T. R., Kujawa, C., Gaete, A., and Franco-Marin, L. (2017). Thermal and gas dynamic investigations at Lastarria volcano, Northern Chile. The influence of precipitation and atmospheric pressure on the fumarole temperature and the gas velocity. *J. Volcanol. Geotherm. Res.* 346, 134–140. doi:10.1016/j.jvolgeores.2017.03.013